Polarization Dynamics of Optically Pumped VCSELs

A. Gahl, S. Balle, and M. San Miguel

[*] [†]

Abstract

We consider the polarization dynamics of optically pumped vertical–cavity surface–emitting lasers (VCSELs) with a pump light of arbitrary polarization ellipticity. We also consider the effect of an applied transverse magnetic field on the polarization properties of the output light. We first test our theoretical description by analyzing the polarization state of the photoluminescence light emitted by an optically pumped quantum well, and discuss a variety of phenomena known to be originated by spin carrier dynamics in these materials. We discuss how these phenomena are modified when a VCSEL is operated above threshold and we show that our model gives a good description of Larmor oscillations observed in VCSELs excited with short optical pulses. For VCSELs under continuous optical pump we find a number of accessible experimental situations in which self-sustained polarization oscillations in the emitted light are possible. We identify and analyze three different mechanisms for these oscillations to occur. When no magnetic field is applied we find polarization oscillations governed by birefringence, and undamped polarization oscillations at the relaxation oscillation frequency. With an applied magnetic field we find self-sustained oscillations governed by the Larmor frequency. In addition our study of optically pumped VCSELs makes apparent the effects of spin carrier dynamics in the polarization properties of the emitted light.

Keywords: VCSEL, QW, polarization, Larmor oscillation, Hanle effect

---

[*]This work was supported by the European Union under Project FMRXCT 96–066 and by CICYT, Spain, under Project TIC95–0563.

[†]A. Gahl, S. Balle, and M. San Miguel are with the Instituto Mediterraneo de Estudios Avanzados, IMEDEA (CSIC-UIB), E–07071 Palma de Mallorca, Spain.

Typeset using REVTEX

I. INTRODUCTION

The polarization state of laser light is generally determined by the combined effects of linear cavity anisotropies, such as birefringence and dichroism, and by the nonlinear gain properties of the stimulated emission process. The polarization state is usually well stabilized in conventional edge-emitting laser diodes in which cavity effects dominate. However, the special geometry of vertical–cavity surface–emitting lasers (VCSELs) leads to a number of polarization instabilities in which nonlinear gain properties are expected to play a more important role. Electrically pumped VCSELs tend to emit linearly polarized light along one of two preferred axis. As the current is increased, a switching in the polarization state [1,2] is often observed with no change in the emission profile which corresponds to the fundamental transverse mode. For higher currents, polarization instabilities become correlated with changes in the emission profile [2–4].

The Spin Flip Model (SFM) [5] for the polarization dynamics of Quantum Well (QW) VCSELs has been a useful instrument to describe a number of polarization properties of VCSELs [6–16] including polarization fluctuations [17] and polarization selection of higher order transverse modes [18,19]. In particular, it satisfactorily describes observations of a polarization switching [20] which is not just caused by thermal heating effects [21,22] or linear cavity anisotropies [23].

A basic feature of the SFM model is that the dominant electron–hole recombination in the QW between conduction and heavy hole bands occurs through two distinct carrier densities. The two carrier densities are associated with spin–up and spin–down and they are coupled by spin–flip processes which tend to equalize the two carrier densities. Recombination of electrons with spin-up or spin-down gives rise to two lasing transitions associated with right– or left–handed circularly polarized emission, which are coupled through birefringence. Under electrical pumping the two transitions are equally pumped, and birefringence leads to the phase locking of the two circular polarizations, thus yielding linearly polarized emission oriented along one of the preferred cavity axes.

In this paper we will consider a non-resonant optical pump, so that by changing the pump ellipticity one can selectively favor one of the two lasing transitions. We explore how, in this situation, oscillations in the polarization of the emitted light can appear through the coupling of the two transitions. Applying a transverse magnetic field forces the carriers' spin to precess, and this provides and additional coupling mechanism that we will consider. We find a number of experimentally accessible situations in which self-sustained polarization oscillations are possible.

Favoring one of the two lasing transitions by optically pumping the VCSEL is a useful way to unmask the spin carrier dynamics. This procedure has been extensively used to study the effects of spin flip processes in QW semiconductor materials through polarization and time resolved photoluminescence (PL) and absorption experiments, and time resolved magneto-optical techniques [24–32]. It has also been used to study the polarization dependence with magnetic field strength under continuous optical excitation (Hanle effect) [33,34]. These studies yield values for the characteristic time of spin relaxation which typically range from about 10 ps at room temperature to 200 ps at low temperature [28,32,35], although electron spin lifetimes of nanoseconds have been measured [30,31]. The consideration of carrier spin dynamics opens the possibility of fast all-optical switches based in the polarization state of light [36] and also the possibility of coherent quantum semiconductor devices.

A question that we address in this paper is how those effects of spin dynamics are modified when considering the QW material in an optical cavity above the lasing threshold. The value of the characteristic time for spin relaxation is also expected to be different. The predictions of the SFM model are sensitive to the value of this parameter. In particular, for vanishingly short spin relaxation time, the densities of spin-up and spin-down carriers are always equal and no influence of the carrier's spin dynamics is expected. Therefore, a number of proposals and experiments on electrically pumped VCSELs have already been made to determine the actual value of the spin-flip rate under lasing conditions at room temperature. One is based on measuring the effect of a longitudinal magnetic field on the ellipticity of the emission due to the Zeeman splitting of the magnetic sublevels [8–10]. Another one is based in the fitting of results for a polarization switching at constant temperature [20,37]. Other measurements [17] are based on the fluctuations of the ellipticity and the polarization direction [12,13] or the red-shift of the spontaneous emission peak of the off-mode in the field spectrum of linearly polarized emission [7,11]. These studies give an estimate of the characteristic time of spin relaxation in the range of 1-15 ps. The consideration of optically pumped VCSELs offers much more flexible opportunities to determine this characteristic time, as for example the recent proposal based on the analog of the Hanle effect for a VCSEL [38].

The paper is organized as follows. We first summarize in Section II an extension of the SFM model that describes the polarization dynamics of optically pumped VCSELs taking also into account a possible applied transverse magnetic field. The model is tested in Section III by analyzing the time-resolved photoluminescence and the Hanle effects associated with carrier spin dynamics in QW material. We show that these phenomena are well described by our general model in the limiting case of very bad laser cavity. In Section IV we show how these phenomena are modified in VCSELs due to nonlinear gain dynamics above the lasing threshold [39,40]. In particular we show that our theoretical framework gives a good description of recently observed Larmor oscillations in VCSELs excited with short optical pulses [39], and we discuss what information about the carriers' spin dynamics can be obtained from them. In Section V we analyze different situations in which self-sustained polarization oscillations could be observed under continuous optical excitation of a VCSEL. We identify and analyze three main scenarios: birefringence activated polarization oscillations, oscillations occurring through the undamping of relaxation oscillations, and oscillations governed by Larmor precession. These self-sustained polarization oscillations could be useful for optical clock generation. Section VI contains a summary of our conclusions.

II. MODEL FOR POLARIZATION DYNAMICS IN OPTICALLY PUMPED VCSELS

A model that takes into account the effect of spin dynamics of the carriers in the polarization properties of QW VCSELs was first proposed in [5]. This model can be extended to describe the effect of different pump polarizations in optically pumped VCSELs, as well as to incorporate the influence of an arbitrary magnetic field on the spin dynamics [38].

Fig. 1 depicts the main ingredients of the model which features two coupled lasing transitions associated with right (E_+) and left (E_-) circularly polarized output fields: The magnetic structure of the conduction band in the vicinity of the band edge corresponds to an angular momentum $J_z = \pm 1/2$, the magnetic structure of the heavy–hole valence band corresponds to an angular momentum $J_z = \pm 3/2$. Thus, the predominant electron–hole recombination in a QW yields E_+ resp. E_- polarized light fields which are coupled by the crystal birefringence γ_p. In addition to this coherent coupling of the fields, the lasing transitions are also coupled through carrier spin dynamics. This includes spin relaxation processes characterized by a decay rate γ_s and the effect of externally applied magnetic fields. We will consider here the Voigt geometry in which magnetic field with characteristic Larmor frequency Ω_x is applied in the plane of the QW (transverse to the output direction) .

We consider a non-resonant optical pump whose ellipticity can be used as a tuning parameter to pump in different amounts the two lasing transitions. The pump field and the VCSEL field will not be coherently coupled if the pump light is strongly detuned to the blue of the cavity resonance of the VCSEL. Because the electron spin direction remains almost unchanged during the fast relaxation process towards the low energy edge of the conduction band [26], the polarization ellipticity of the pump field is transferred into a corresponding population difference in the electron densities of the two spin subbands of the conduction band. Any difference in these electron densities results in a non–vanishing longitudinal component m_z of an electron spin magnetization $\vec{m}$. The electron spins, and therefore the magnetization, precess in an applied transverse magnetic field B_x yielding a coherent coupling of the spin subbands. Additionally, an incoherent coupling results from spin–flip processes, characterized by the magetization decay rate γ_s.

The magnetization of the valence band can be neglected because the heavy holes lose their spin orientation much faster than the electrons in the conduction band [35]. Therefore, we treat the heavy–hole subbands as equally populated.

The physical mechanisms described above are included in the following model equations for the fundamental transverse mode operation of a VCSEL which also take into account saturable dispersion and the effect of cavity anisotropies [5,6,38]

$$\dot{E}_\pm = \kappa(1+i\alpha)(N \pm m_z - 1)E_\pm - (\gamma_a + i\gamma_p)\, E_\mp + \sqrt{\beta\gamma(N \pm m_z)}\xi_\pm \tag{1}$$

$$\dot{N} = \gamma\left[\eta_+ + \eta_- - (1 + I_+ + I_-)N - (I_+ - I_-)m_z\right] \tag{2}$$

$$\dot{m}_z = \gamma(\eta_+ - \eta_-) - \left[\gamma_s + \gamma(I_+ + I_-)\right] m_z - \gamma(I_+ - I_-)N + \Omega_x m_y \tag{3}$$

$$\dot{m}_y = -\left[\gamma_s + \gamma(I_+ + I_-)\right] m_y - \Omega_x m_z . \tag{4}$$

In these equations, E_+ and E_- are the slowly varying complex amplitudes of the circularly polarized components of the normalized electric field, and $I_\pm = |E_\pm|^2$ are the corresponding intensities; β is proportional to the fraction of spontaneous emission noise that ends up in the laser mode; $\xi_\pm$ are complex Gaussian white noise sources of zero mean value and δ–correlated in time [41]; η_+ (η_-) is the optical pump of the E_+ (E_-) component; N is the normalized total electron density whose decay rate is γ; the electron magnetization $\vec{m}$ has a decay rate γ_s due to spin–flip processes and electron–hole recombination; the Larmor frequency Ω_x is proportional to the transverse magnetic field strenght B_x; κ is the cavity decay rate; α is linewidth enhancement factor; γ_p is the linear birefringence, and γ_a is the gain anisotropy.

For further use we introduce a number of additional variables: the total pump $\eta = \eta_+ + \eta_-$, and the pump ellipticity

$$P = \frac{\eta_+ - \eta_-}{\eta_+ + \eta_-}\ , \tag{5}$$

the total intensity $I = I_+ + I_-$ of the VCSEL emission and its ellipticity

$$\epsilon = \frac{I_+ - I_-}{I_+ + I_-}\ . \tag{6}$$

Note that for $P = 0$ one formally reproduces the situation of an electrically pumped VCSEL, and for both $P = 0$ and $B_x = 0$ we recover the set of equations considered in [5,6].

As already commented, the role of the transverse magnetic field is to induce a periodic transfer of carrier density from one spin subband to the other by means of Larmor precession, thus coherently coupling them. When $B_x = 0$, the electron spins do not precess, and therefore the magnetization vector $\mathbf{m} = (0, m_y, m_z)$ decays without precession, i. e. it keeps its orientation. Hence, in atomic language the magnetization vector describes the coherence of the two conduction spin subbands, while the total carrier density N corresponds to the degree of excitation of the transition. The sources for the magnetization are both the ellipticity of the pump beam and differences in the intensities of the lasing transitions, which yield different stimulated emission rates for the conduction spin subbands thus leading to different carrier density in each channel. The decay rate of the magnetization is $\gamma_s + \gamma(I_+ + I_-)$, i. e., it increases with the total intensity of the optical field.

It is important to note that the typical decay time for the carrier spin dynamics in the QW is determined by γ_s^{-1}, which, as indicated previously, usually ranges from a few ps to 200 ps [35,28,32]. Thus the decay of the coherence among the spin subbands is typically quite faster than the decay of the degree of excitation of the transition ($\gamma^{-1} \approx 1$ns), but it is in general slower or comparable to the lifetime of the photons in the VCSEL cavity, $(2\kappa)^{-1} \approx 5$ps, so that carrier spin dynamics cannot be disregarded in polarization dynamics of VCSELs.

III. SPIN RELAXATION AND POLARIZATION PROPERTIES OF QWS

Spin relaxation processes have been widely studied in bulk and QW semiconductor materials [33,35]. In particular, a large number of results are available from absorption and PL experiments [24–26,28,32] as well as from the observation of Larmor oscillations [26,27]. In addition, the Hanle effect [33,34] gives a classical measure of the spin decay rate. As a first step towards the understanding of the effect of spin carrier dynamics in VCSELs we consider here how the available experimental results on polarization properties of optically driven semiconductor QWs are well reproduced within the general scheme of Eqs. (1)–(4). To this end we treat the QW as a low–Q cavity VCSEL in which the lasing threshold is not reached. The photon lifetime in a QW corresponds to $\kappa \approx (10\text{fs})^{-1}$, which becomes much larger than the other time constants, thus allowing for the adiabatic elimination of the light field. Because the pump level is far below threshold, $|N \pm m_z| \ll 1$, and because of $|\kappa| \gg |\gamma_p/\alpha|, |\gamma_a|$ the effects of the anisotropies can be neglected. With these approximations we obtain for the intensities

$$I_\pm = 2\beta\frac{\gamma}{\kappa}(N \pm m_z) \tag{7}$$

Under this conditions $I_\pm$ are sufficiently small to be neglected in the dynamical equations for N and $\vec{m}$:

$$\dot{N} = \gamma\left(\eta_+ + \eta_-\right) - \gamma N \tag{8}$$

$$\dot{m}_z = \gamma(\eta_+ - \eta_-) - \gamma_s m_z + \Omega_x m_y \tag{9}$$

$$\dot{m}_y = -\gamma_s m_y - \Omega_x m_z. \tag{10}$$

The proportionality of I_+ and I_- to the corresponding spin subband populations $N + m_z$ and $N - m_z$ provides insight into the spin dynamics by means of polarization–resolved investigations of the PL.

A. Photoluminescence and Larmor Oscillations

In polarization– and time–resolved PL spectroscopy the QW is excited with a short, circularly polarized pulse. To describe the polarization resolved PL signals as they have been measured, for example, in [25] for $B_x = 0$, we solve the full set of eqs. (1)–(4) with a Gaussian pulse

$$\eta(t) = \hat{\eta}\exp\left[-2\left(\frac{t}{\tau}\right)^2\right] \tag{11}$$

where τ is the pulse length and $\hat{\eta}$ is the maximum pump.

Fig. 2 shows our results which compare well to the low temperature experiments ($\gamma_s/\gamma = 5$) of [25]. Fig. 2a) shows the PL signals I_+ and I_-, while Fig. 2b) shows the corresponding spin band populations $N + m_z$ and $N - m_z$. The short, circularly polarized pulse populates only the spin band which gives rise to I_+ PL. Then, spin–flip processes start equalizing the population of the spin bands leading to an increase of I_- PL resulting eventually in an equalization of both PL signals. From the decay of the $I_+ + I_-$ resp. $I_+ - I_-$ signal one can extract γ resp. γ_s, since τ is small compared with γ^{-1} and γ_s^{-1}.

When a transverse magnetic field is applied, damped and antiphase oscillations of the PL signals I_+ and I_- at the Larmor frequency have been observed [26,27]. These observations are also well reproduced by a numerical integration of eqs. (1)–(4) as shown in Fig. 3. Fig. 3a) shows the PL signals while Fig. 3b) shows the corresponding spin subband populations. The short optical pulse populates only one spin subband creating a definite magnetization m_z, but the transverse magnetic field B_x forces the magnetization to precess in the z–y–plane, as described by eqs. (9)-(10). Therefore, the populations of the electron spin subbands oscillate with the Larmor frequency Ω_x, which in turn, as follows from eq. (7) , leads to an oscillation of I_+ and I_- with Ω_x. The damping rate of these oscillations can be also used as an indirect measurement of γ_s.

These Larmor oscillations have been also termed "quantum beats" [26,27] since they could be interpreted as the damped quantum evolution of the state created by the optical pulse. This state is a coherent superposition of the two eigenstates of the Hamiltonian associated with the transverse magnetic field. The oscillation frequency is the frequency beat between these two eigenstates. Regardless of the interpretation, the observation of these oscillations requires excitation with optical pulses short compared with the spin relaxation time γ_s^{-1}. Under continuous optical excitation one spin subband is being continuously populated and Larmor oscillations are not observed in a QW. We will discuss in Sect. V how additional coupling mechanisms present in a VCSEL permit to sustain Larmor oscillations under continuous optical excitation.

B. Hanle Effect

Spin relaxation processes result in another well known effect, the Hanle effect, when a semiconductor material is continuously excited in a transverse magnetic field, but now with elliptically polarized light: both in bulk semiconductors [33] and QWs [34] the degree of polarization $|\epsilon|$ of the PL decreases with increasing transverse magnetic field strength.

This effect is easily described within the approximation of Eqs. (7)–(10). Their steady state solutions yield

$$|\epsilon| = \left|\frac{m_z}{N}\right| = |P| \, \frac{\gamma}{\gamma_s} \, \frac{1}{1 + (\Omega_x/\gamma_s)^2}. \tag{12}$$

Therefore, the PL polarization is proportional to the pump polarization, but there is a Lorentzian–shaped decrease of $|\epsilon|$ with increasing Larmor frequency $|\Omega_x|$. This can be interpreted in terms of an effective magnetization decay rate $\gamma_s + \Omega_x^2/\gamma_s$ caused by the spin band mixing under the influence of the transverse magnetic field. A Lorentzian fit of this decay has been used for the determination of γ and γ_s [33,34].

IV. POLARIZATION PROPERTIES OF OPTICALLY PUMPED VCSELS

We now address the question of how the polarization properties of sub-threshold laser light observed in QW materials and described above are modified in a VCSEL above thresh-

old. The existence of net gain in the cavity deeply modifies the physical processes. In particular, the proportionality of I_+ and I_- to the corresponding spin band populations (eq. (7)) is obviously lost. The much higher density of carriers in the cavity is expected to lead to significant changes in the value of γ_s. Therefore, it has to be checked, if any of the previously discussed indirect methods of measurement of γ_s is still useful to determine γ_s under lasing conditions. Additionally, in the situation above threshold cavity anisotropies can no longer be neglected. Especially, birefringence provides an important coupling mechanism between the two polarized components of the field which was absent in the QW description.

A. Pulsed excitation and Larmor oscillations

Larmor oscillations in stimulated emission of light in an optically pumped VCSEL at low temperatures have been recently observed. A theoretical description of these observations has been given using a detailed microscopic theory of the many body semiconductor physics [39]. We show here how these observations are satisfactorily explained within our model eqs. (1)–(4) which account for the main physical mechanisms relevant for this phenomenon. We follow the experimental conditions of low temperature ($\gamma_s/\gamma = 5$), pulse length of 2ps, elliptically polarized pump ($P = 0.5$) and magnetic fields of a few Tesla ($\Omega_x/B_x = 2\pi \times$ 5.5GHz/T).

We first consider the response of the VCSEL to the optical pulse for $B_x = 0$: Fig. 4 shows the temporal evolution of the VCSEL emission and the spin band populations. About 50 ps after the pump pulse has been applied, the VCSEL emits a pulse of I_+ light which grows from the noise level. 20 ps later, stimulated emission starts depleting the gain which turns into absorption after 10 ps more, thus yielding a VCSEL pulse of $\sim$ 30 ps duration emitted $\sim$ 80 ps after the pump pulse has been applied.

Since there is absorption for I_- light at any time, the VCSEL emission is almost circularly polarized although the pump polarization is $P = 0.5$. This is a main difference with the PL experiments in QWs in which there is a tendency to equalize the intensity of the two polarized PL signals (see Fig. 2a). The nonlinearity of the stimulated emission process gives strong amplification of the preferred polarization component and absorption of the other one. Only one of the two lasing transitions is activated with emission of a pulse of circularly polarized light and no information is obtained on coupling mechanisms such as γ_s.

Fig. 5 shows the temporal evolution of the VCSEL emission and the spin band populations when a transverse magnetic field is applied. These results give a good description of the experimental observations in [27,39]. The main effect of applying a transverse magnetic field is to give an efficient mechanism to couple the two lasing transitions. The fast Larmor oscillation in the carrier populations (magnetization precession) results in short periods of amplification followed by absorption ones, so that the intensities never reach a level high enough to deplet the gain significantly by stimulated emission. This is clearly seen comparing the peak values of the intensity in Fig. 4 and Fig. 5. The consequence is that oscillations in the polarization of the emitted light are still observed. We note that the additional coupling due to birefringence is not important in this situation, but its effect is still seen by the fact that at the time that one polarized intensity reaches its maximum, the other polarized intensity has a small nonvanishing value.

The damping of the oscillations of $N \pm m_z$ gives in principle information on the decay rates γ and γ_s. However, in contrast to the QW case this information can not be extracted from the experimental observation of the emitted light since intensities and the corresponding spin band populations are no longer proportional. However, a precise determination of the Larmor frequency is still possible.

For the same reasons than in the QW case, the observation of Larmor oscillations require a small value of γ_s. At room temperature, where one usually finds $\gamma_s > |\Omega_x|$ Larmor oscillation are strongly damped out so that only one single peak would appear. Grossly speaking, doubling the value of γ_s due to an increase of temperature reduces the number of visible peaks to the half. Additionally, the observation of Larmor oscillations in a VCSEL require that there is no complete gain depletion of one of the lasing transitions. This is achieved in the example of Fig. 5 thanks to the elliptical polarization of the pump. If the

pump is circularly polarized a much more intense first pulse of light is emitted and the oscillations are erased by gain depletion. However, the oscillations can be recovered by lowering the maximum power of the circularly polarized pump.

B. Hanle effect

We next consider the polarization properties of the light emitted by a VCSEL which is continuously pumped with ellipticaly polarized light in a transverse magnetic field. From the steady state solution of eqs. (1)–(4) we find that the degree of polarization $|\epsilon|$ of the VCSEL emission also decreases with increasing strength of a transverse magnetic field, but now also under lasing conditions ($\eta > 1$) (see Fig. 6).

In contrast to the QW case where $|\epsilon|$ depends on the spin band population ellipticity m_z/N but not on anisotropies, the latter ones come into play in the VCSEL case. For very small cavity anisotropies (e.g. for $|\gamma_p| \ll |\kappa\alpha m_z|$) a non–vanishing magnetization m_z, introduced by an elliptically polarized optical pump, would result in almost circularly polarized emission $|\epsilon| \to 1$. In this regime, $|\epsilon|$ is almost insensitive to the magnetic field strength.

However, in the regime of large cavity anisotropies (e.g. for $|\gamma_p| \gg |\kappa\alpha m_z|$) a Lorentzian–shaped decrease of $|\epsilon|$ occurs for $I \ll \gamma_s/\gamma$ and $\epsilon^2 \ll 1$, conditions that can be experimentally achieved by operating close above threshold ($\eta - 1 \ll \gamma_s/\gamma$) and, if necessary, by decreasing the degree of the pump polarization $|P|$. Using the approximation $|\gamma_a| \ll |\gamma_p|$, which is usually valid in VCSELs, we find above threshold ($N \approx 1$)

$$|\epsilon| \approx \left|\frac{\kappa\alpha m_z}{\gamma_p}\right| \approx |P|\ \eta\ \frac{\gamma}{\gamma_s}\ \frac{\kappa\alpha}{|\gamma_p|}\ \frac{1}{1+(\Omega_x/\gamma_s)^2}. \tag{13}$$

Measuring the width Ω_x/γ_s of the Lorentzian allows for the determination of γ_s in VCSELs under lasing conditions, even without knowing $P, \eta, \kappa, \alpha, \gamma, \gamma_p, \gamma_a$ precisely [38]. From values of γ_s and Ω given in [10] one can estimate that a magnetic field strength of the order of 10T is required for the determination of γ_s at room temperature using the Hanle effect.

V. POLARIZATION OSCILLATIONS IN CONTINUOUSLY PUMPED VCSELS

The oscillatory phenomena discussed so far are the result of transients after an optical pump pulse is applied to the VCSEL. The oscillations originate from Larmor precession of the carriers' spins due to the transverse magnetic field, which leads to oscillations of the polarization of the emitted light. These oscillations are damped due to spin-flip processes mainly, hence they vanish after a short transient.

However, the description of the VCSEL in terms of two nonlinearly coupled subsystems (each of them defined by a circular polarization component of the optical field and the carrier density with the corresponding spin orientation, see Fig. 1) indicates the possibility of self-sustained oscillatory behaviour. In fact, each of the two subsystems behaves like a damped oscillator when isolated from the other, the oscillation frequency being the relaxation oscillation one, around a carrier frequency determined by the α factor and the threshold carrier density for each subsystem. Birefringence and an external magnetic field couple the two subsystems in an oscillatory fashion (birefringence induces a back and forth transfer of circularly polarized light, while the external transverse magnetic field leads to spin precession which produces a periodic transfer of spin density —and hence gain— from one channel to the other). On the other hand, spin-flip processes tend to equalize the gain for both channels, while dichroism tries to equalize the field amplitude in each channel. Therefore, for a steady state to develop, it is required that the nonlinearities in the system force the phase locking of the two circularly polarized components of the optical field, i. e., that the two circular components have the same frequency and a maintain a constant phase difference. The range of existence and stability of such phase-locked states depends on the control parameters of the system (η and P), so that when the system is brought outside the stable locking-range a dynamical state occurs.

In certain parameter regions, it can be expected that nonlinear coupling among the two subsystems can then produce the unstabilization of any of the natural oscillations present in the system (birefringence oscillations, naturally damped by dichroism; Larmor oscillations, naturally damped by spin-flip; or relaxation oscillations, naturally damped by the carrier lifetime) by means of harmonic or beat note excitation, thus leading to self-sustained oscillations in the polarization of the emitted light even for CW pumped VCSELs.

Such self-sustained polarization oscillations would be quite interesting from a practical point of view in order to achieve optical clock generation, especially if the oscillation frequency could be tuned by some means. It would be particularly relevant that the oscillations occur at room temperature and without requiring an intense transverse magnetic field.

A quantitative analysis of the onset of the oscillations (and its frequency) as a function of the system parameters requires a rather involved linear stability analysis of eqs. (1 - 4) along the lines of the one performed in [10]. However, some qualitative understanding can be gained by simply considering the conditions for the existence of elliptical solutions in the absence of an externally applied magnetic field. Such solutions are characterized by a constant phase difference, ψ, among the two circular components of the optical field, and they exist over the range of parameters (η, P) for which the system of equations

$$sin\psi \; cos\psi = \frac{m_z}{N-1} \frac{\gamma_a\gamma_p - \alpha\kappa^2\left[(N-1)^2 - m_z^2\right]}{\gamma_a^2+\gamma_p^2} \;, \tag{14}$$

$$tan\psi = \frac{\gamma_a}{\gamma_p} \frac{(\eta-N)m_z + \left[N(N-1) - m_z^2\right](\eta P - \Gamma m_z)}{(\eta - N)\left[N(N-1)-m_z^2\right] + m_z(\eta P - \Gamma n)} \;, \tag{15}$$

$$m_z^2 = (N-1)^2 + \left(\frac{\gamma_p}{\kappa}\right)^2 sin^2\psi - \left(\frac{\gamma_a}{\kappa}\right)^2 cos^2\psi \;, \tag{16}$$

with $\Gamma = \gamma_s/\gamma$, has solutions with non-zero intensities, i. e.,

$$I_\pm = \frac{\eta - N \pm (\eta P - \Gamma m_z)}{2(N \pm m_z)} > 0 \;. \tag{17}$$

An approximate solution to equations (14-17) can be found when birefringence dominates over dichroism, i. e., $\gamma_a << \gamma_p$. In this case we have that, to order γ_a/γ_p, the solutions are approximately given by

$$N \sim 1 \pm \frac{\gamma_a}{\kappa} \;,$$
$$m_z \sim \frac{\eta P}{\Gamma} \;,$$
$$sin\psi \sim 0 \;,$$

$$I_\pm = \frac{\eta - N}{2(N \pm m_z)} \ .$$

These states have a weak ellipticity due to the ellipticity of the pump beam, which yields different intensities for the two circularly polarized components of the optical field, and they develop from the linearly polarized solutions characteristic of the case $P = 0$. From the expressions for the intensities of the circularly polarized components it is clear that the ellipticity of the pump beam sets an upper limit for the existence of such solutions,

$$\eta_c \sim \frac{\Gamma}{|P|}\left(1 \pm \frac{\gamma_a}{\kappa}\right) \ ,$$

the limit being lower for either higher ellipticity of the pump beam or lower values of Γ; hence we expect their stability range to reduce accordingly. We note that, in the previous analysis, we have considered that neither γ_a nor γ_p vanish. In the special case where one or both of these paramenters vanish, other elliptical solutions arise [6,9,10] which cannot be obtained by cancelling terms in the approximate solutions above.

The former analysis, although being qualitative, indicates that the VCSEL may reach an oscillatory state. Moreover, it also suggests that such oscillatory states should occur closer to threshold when using an elliptical pump beam or when the VCSEL is operated at low temperature, since in both cases the existence regime shrinks —in the first case, due to the larger value of P, and in the second, due to the smaller value of γ_s. The numerical study presented in the next subsections shows that this is indeed the case, and in the following we present the different scenarios for these oscillations to occur and the mechanisms leading to them. In all these cases we find that polarization oscillations having frequencies ω_p that are not at least of the order of γ_s are strongly damped out by spin-flip processes so that self–sustained polarization oscillations have a minimum frequency governed by the spin–flip rate.

A. Birefringence Governed Oscillations

The first mechanism for self-sustained polarization oscillations is associated with birefringence. As already commented, birefringence leads to an oscillatory transfer of power among the two circular polarization components of the emitted light. For the steady state to develop, the nonlinearities impose a phase-locking of the two circular components which in the cases where the two spin channels are equally pumped (i. e., for electrical pumping or for optical pumping with a linearly polarized field) in general leads to linearly polarized light. However, the locking range and the locking phase depend on the pump level and the anisotropies of the VCSEL cavity, thus increasing the pump level may lead to polarization instabilities, such as polarization switching, elliptically polarized emission (characterized by a non vanishing magnetization) or dynamical states when the pump level trespasses the locking range [6,9]. It is worth noting that even though the externally induced magnetization is zero, steady states with definite ellipticity can arise as the locking phase of the two circularly polarized components changes.

When an optical pump of arbitrary ellipticity is considered, a state with non vanishing magnetization m_z is externally favoured. Hence, from the point of view of the circular components of the optical field, the birefringence is coupling two detuned fields, with a frequency difference given by

$$\Delta\omega_\pm = 2\kappa\alpha m_z. \qquad (18)$$

The phase locking process described above still takes place, leading to the emission of elliptically polarized light. However, we expect the locking range to be reduced due to the frequency detuning of the two circularly polarized components, leading to the onset of self-sustained oscillations.

In Fig. 7 we show two different cases where birefringence oscillations appear. The right column of Fig. 7 corresponds to a linearly polarized optical pump in the low temperature regime. This case corresponds to the unstabilization of the elliptical states discussed in

[6,9] which have a dynamical origin. It is worth noting that the larger the value of γ_s, the higher the pump level required in order to generate this elliptical state, and hence to unstabilize it. However, the larger restoring effect towards nearly linear emission associated with larger γ_s can be compensated with the ellipticity of the pump beam, which naturally favours elliptically polarized states which then may become unstable (see left column in Fig. 7). It is worth remarking that no transverse magnetic field is required in any case, and that these oscillations can be excited even at room temperature (left column in Fig. 7) for strong ellipticity of the pump beam. This control parameter allows for the observation of these type of oscillations in much wider parameter regimes in comparison with the case in which the VCSEL is pumped electrically or with linearly polarized light.

The frequency of the polarization oscillations is given by

$$\omega_p \approx \sqrt{4\gamma_p^2 + (\Delta\bar{\omega}_\pm)^2} \tag{19}$$

where $\Delta\bar{\omega}_\pm$ is the time–averaged value of $\Delta\omega_\pm$. It is found that a necessary condition for these oscillations to become excited is that

$$|\Delta\bar{\omega}_\pm| \approx |\gamma_p| \,,$$

while $\omega_p \approx \gamma_s$. This condition is the statement of a quasi-resonance between the birefringence and the equivalent circular birefringence associated with the non vanishing magnetization m_z that can not be any longer damped by spin-flip processes, thus breaking the phase-locking condition that leads to a steady state. Since room temperature values for γ_s are quite large, strong ellipticity of the pump beam and high pump levels are required to excite these oscillations. The quasi-resonance condition implies that the oscillation frequency is barely tunable, but it turns out to be quite robust against changes in either ambient conditions or ellipticity of the pump beam.

B. Activation by Relaxation Oscillations

Another mechanism for the appearence of self-sustained polarization oscillations is associated with the undamping of the relaxation oscillations of the system. In Fig. 8 where we depict the time series of the total intensity as we change the pump level while keeping its ellipticity $P = 0.5$. At $t = 0$ the pump level η is increased to a value that finally leads to stable emission. After reaching the stable emission state, at $t = 5$ ns the pump level is further increased leading to oscillations in both the total intensity and in the polarization state of the output light. The oscillation frequency is that of the relaxation oscillations, Ω_R (compare Fig. 8b to Fig. 8c), which becomes undamped.

Our interpretation of the undamping mechanism is a quasi-resonance mechanism analogous to the one discussed in the previous subsection. In the present case, the pump beam polarization P is such that it tends to create a time–averaged magnetization $\bar{m}_z$ that closely matches the beat frequency $\Delta\bar{\omega}_\pm$ to the frequency of the relaxation oscillations. Actually, Fig. 8b clearly shows that the weaker polarization component is feeded through a nonlinear four-wave mixing mechanism on its low frequency side-band.

It is worth noting that these oscillations can occur only at low temperatures, where it is feasible to have $\Omega_R > \gamma_s$. However, they do occur in the absence of transverse magnetic field. In the present case, the oscillation frequency can be moderately tuned by control of the pump level and polarization, but careful matching of the two parameters is required.

C. Self–Sustained Larmor Oscillations

Finally, in the presence of a transverse magnetic field, nonlinear coupling among the two channels may lead to the undamping of the spin precession, thus leading to polarization oscillation whose frequency is governed by the Larmor frequency, as shown in Fig. 9.

In the case shown in this figure, the magnetization $\vec{m}$ precesses in the z–y–plane at the Larmor frequency which is very close to the third harmonic of the birefringence. Hence, the third harmonic of the damped birefringence oscillations feed oscillations at the Larmor frequency which become undamped. Noteworthy, the frequency of these oscillations can be easily tuned by varying the magnetic field strengh or the pump level, and as shown in the picture, these oscillation may occur even for a linearly polarized pump beam. However, they require the system to be operated at low temperatures, since a necessary condition for these oscillations to occur is that $|\Omega_x| > \gamma_s$, which requires a huge magnetic field at room temperature.

An important characteristic of these oscillations is that, for fixed magnetic field strentgh, they exist in a range of values for γ_p such that Larmor frequency is close to a harmonic of the birefringence. Lowering or increasing the birefringence outside this range leads to the suppression of the oscillation.

However, in all cases studied we observe a maximum oscillation frequency $\nu_{\max}$ which strongly depends on the cavity losses, κ. For fixed pump level we find

$$\nu_{\max} \sim \sqrt{\kappa}\ , \tag{20}$$

which can be interpreted as the cavity acting as a low-pass filter. In addition, this maximum value for the oscillation frequency also indicates that these oscillations cannot be observed at room temperature, since in this limit we have $\gamma_s \gg \sqrt{\kappa}$. As a consequence, the oscillations are damped, and we are left with the Hanle effect discussed in Sect. IV. On the other hand, for fixed cavity loss we find that the maximum frequency can also be controlled by changing the pump level, although to a much lesser extent (see Fig. 10b). The existence of a maximum oscillation frequency $\nu_{\max}$ and its sensitivity to these two parameters has been observed experimentally and it has also been found in numerical simulations from a first–principle model [39,40]. However, further investigation of the mechanisms leading to a maximum value of the oscillation frequency are required.

VI. SUMMARY AND CONCLUSIONS

We have examined the polarization dynamics of the light emitted by optically pumped VCSELs in a transverse magnetic field. The VCSEL is described by the spin-flip model [5], extended to take into account non-resonant optical pump and the effects of the magnetic field. The model is tested by considering the bad cavity limit, which allows us to satisfactorily describe the experimentally observed features of polarization dynamics in QW systems in both pulsed and CW operation. For an optically pumped VCSEL, Larmor oscillations are found under pulsed operation at low temperature, in agreement with recent experimental observations. For CW pump, we find that Hanle effect provides a convenient method for measuring the spin relaxation rate under lasing conditions at room temperature. We have shown the possibility of generating self-sustained polarization oscillations that might be suitable for optical clock generation. Three different oscillation mechanisms have been identified, namely, birefringence activated polarization oscillations, oscillations occurring through the undamping of relaxation oscillations, and oscillations governed by Larmor precession. The dynamical origin and control characteristics of these three types of polarization oscillations have been examined. In particular, we have shown that birefringence governed oscillations of the polarization are possible at room temperature and with no applied magnetic field.

REFERENCES

[1] Z.G. Pan, S. Jiang, M. Dagenais, R.A. Morgan, K. Hojima, M.T. Asom, and R.E. Leibenguth, "Optical injection induced polarization bistability in vertical–cavity surface–emitting lasers," *Appl. Phys. Lett.*, vol. 63, pp. 2999–3001, 1993.

[2] K.D. Choquette, K.L. Lear, R.E. Leibenguth, and M.T. Asom, "Polarization modulation of cruciform vertical–cavity laser diodes," *Appl. Phys. Lett.*, vol. 64, pp. 2767–2769, 1994.

[3] C.J. Chang-Hasnain, J.P. Harbison, G. Hasain, A.C. Von Lehmen, L.T. Florez, and N.G. Stoffel, "Dynamic, Polarization, and Transverse Mode Characteristics of Vertical Cavity Surface Emitting Lasers," *IEEE J. Quantum Electron.*, vol. 27, pp. 1402–1409, 1991.

[4] J.E. Epler, S. Gehrsitz, K.H. Gulden, M. Moser, H.C. Sigg, and H.W. Lehmann, "Mode behavior and high resolution spectra of sircularly–symmetric GaAs–AlGaAs air–post vertical cavity surface emitting lasers," *Appl. Phys. Lett.*, vol. 69, pp. 722–724, 1996.

[5] M. San Miguel, Q. Feng, and J.V. Moloney, "Light–polarization dynamics in surface–emitting semiconductor lasers," *Phys. Rev. A*, vol. 52,pp. 1728–1739, 1995.

[6] J. Martín-Regalado, F. Prati, M. San Miguel, and N.B. Abraham, " Polarization Properties of Vertical–Cavity Surface–Emitting Lasers,"*IEEE J. Quantum Electron.*, vol. 33, pp. 765–783, 1997.

[7] M.P. van Exter, R.F.M. Hendriks, and J.P. Woerdman, "Physical insight into the polarization dynamics of VCSELs,"*Phys. Rev. A*, vol. 57, pp. 2080–2090, 1998.

[8] C. Serrat, N.B. Abraham , M. San Miguel, R. Vilaseca, and J. Martin-Regalado, "Polarization dynamics in a vertical–cavity laser with an axial magnetic field," *Phys. Rev. A*, vol. 53, pp. R3731–3733, 1996.

[9] M. Travagnin, M.P. van Exter, A.K. Jansen van Doorn, and J.P. Woerdman, "Role of optical anisotropies in the polarization properties of surface-emitting semiconductor lasers," *Phys. Rev. A*, vol. 54, pp. 1647–1660, 1996.

[10] A.K. Jansen van Doorn, M.P. van Exter, M. Travagnin, and J.P. Woerdman, "Polarization behavior of surface–emitting semiconductor lasers in an axial magnetic field," *Opt. Comm.*, vol. 133, pp. 252–258, 1997.

[11] H. van der Lem and D. Lenstra, "Saturation–induced frequency shift in the noise spectrum of a birefringent vertical–cavity surface–emitting laser," *Opt. Lett.*, vol. 22, pp. 1698–1700, 1997.

[12] H.F. Hofmann, and O. Hess, "Quantum Noise and Polarization Fluctuations in Vertical Cavity Surface Emitting Lasers," *Phys. Rev. A*, vol. 56, pp. 868–876, 1997.

[13] H.F. Hofmann, and O. Hess, "Polarization fluctuations in vertical–cavity surface–emitting lasers: a key to the mechanism behind polarization stability," *Quantum Semiclass. Opt*, vol. 10, pp. 87–96, 1998.

[14] P. Besnard, F. Robert, M.L. Chares, and G.M. Stephan, "Theoretical modeling of vertical–cavity surface–emitting lasers with polarizaed optical feedback," *Phys. Rev. A*, vol. 56, pp. 3191–3205, 1997.

[15] F. Robert, P. Besnard, M.L. Chares, and G.M. Stephan, "Polarization Modulation Dynamics of Vertical–Cavity Surface–Emitting lasers with an Extended Cavity," *IEEE J. Quantum Electron.*, vol. 33, pp. 2231–2239, 1997.

[16] S.P. Hegarty, G. Huyet, J.G. McInerny, and H. Li. " Polarisation Dynamics and Intensity Noise in VCSELs," *SPIE*, vol. 2994, pp. 190–196, 1997.

[17] M.P. van Exter, A. Al-Remawi and J.P. Woerdman. " Polarisation Fluctuations Demonstrate nonlinear anisotropy of a VCSEL," *Phys. Rev. Lett.*, vol. 80, pp. 4875–4878, 1998.

[18] J. Martin-Regalado, S. Balle and M. San Miguel, "Polarization and transverse mode

dynamics of gain-guided VCSEL," *Opt. Lett.*, vol. 22, pp. 460–462, 1997.

[19] J. Martin-Regalado, S. Balle, M. San Miguel, A. Valle, and L. Pesquera, "Polarization and transverse mode selection in QW VCSELs: index and gain-guided devices," *Quantum and Semiclassical Opt.*, vol. 9, pp. 713–736, 1997.

[20] J. Martín-Regalado, J.L.A. Chilla, J.J. Rocca, and P. Brusenbach, "Polarization switching in vertical–cavity surface emitting lasers observed at constant active region temperature," *Appl. Phys. Lett.*, vol. 70, pp. 3350–3352, 1997.

[21] K.D. Choquette, R.P. Schneider Jr., K.L. Lear, and R.E. Leibenguth, "Gain–Dependent Polarization Properties of Vertical–Cavity Lasers," *IEEE J. of Sel. Topics in Quantum Electron.*, vol. 1, pp. 661–666, 1995.

[22] K. Panajotov, B. Ryvkin, J. Danckaert, M. Peeters, H. Thienpont, I. Veretennicoff, "Polarization Switching in VCSEL's Due to Thermal Lensing," *IEEE Phot. Tech. Lett.*, vol. 10, pp. 6–8, 1998.

[23] A.K. Jansen van Doorn, M.P. van Exter and J.P. Woerdman, "Elasto–optic anisotropy and polarization orientation of vertical–cavity surface–emitting semiconductor lasers," *Appl. Phys. Lett.*, vol. 69, pp. 1041–1043, 1996.

[24] T.C. Damen, L. Vina, J.E. Cunningham, J. Shah, and L.J. Sham, "Subpicosecond spin relaxation dynamics in GaAs quantum wells," *Phys. Rev. Lett.*, vol. 67, pp. 3432–3435, 1991.

[25] S. Bar–Ad, and I. Bar–Joseph, "Exciton Spin Dynamics in GaAs Heterostructures," *Phys. Rev. Lett.*, vol. 68, pp. 349–352, 1992.

[26] A.P. Heberle, W.W. Rühle, and K. Ploog, "Quantum Beats of Electron Precession in GaAs Wells," *Phys. Rev. Lett.*, vol. 72, pp. 3887–3890, 1994.

[27] M. Oestreich, S. Hallstein, and W.W. Rühle, "Spin Quantum Beats in Semiconductors,"

IEEE J. Select. Topics in Quantum Electron., vol. 2, pp. 747–755, 1996.

[28] A. Tacheuchi, Y. Nishikawa, O. Wada, "Room–temperature electron spin dynamics in GaAs/AlGaAs QWs", *Appl. Phys. Lett.*, vol. 68, pp. 797–799, 1996.

[29] S.A. Crooker, J.J. Baumberg, F. Flack, N. Samarth and D.D. Awschalom, "Terahert Spin Precession and Coherent Transfer of Angular Momenta in Magnetic Quantum Wells" *Phys. Rev. Lett.* vol. 77, pp. 2814–2817, 1996.

[30] J.M. Kikkawa, and D.D. Awschalom, "Resonant Spin Amplification in n-type Ga-As" *Science* vol. 277, pp. 1284-1287, 1997.

[31] J.M. Kikkawa, I.P. Smorchkova, N. Samarth and D.D. Awschalom, "Room–temperature Spin Memory in Two-Dimensional Electron Gases" *Phys. Rev. Lett.* vol. 80, pp. 4313–4316, 1998.

[32] R.S. Britton, T. grevart, A. Malinowski, R.T. Harley, P. Perozzo, A.R. Cameron and A. Miller "Room–temperature Spin Relaxation in GaAs/AlGaAs Multple Quantum Wells" *Appl. Phys. Lett.* 1998.

[33] G. Fishman and G. Lampel, "Spin relaxation of photoelectrons in p–type gallium arsenide," *Phys. Rev. B*, vol. 16, pp. 820–831, 1977, and references therein.

[34] M.J. Snelling, G.P. Flinn, A.S. Plaut, R.T. Harly, A.C. Tropper, "Magnetic g factor of electrons in GaAs/Al$_x$Ga$_{1-x}$As quantum wells," *Phys. Rev. B*, vol. 44, pp. 11345 – 11352, 1991.

[35] L.J. Sham, "Spin relaxation in semiconductor quantum wells," *J. Phys. Condens Matter*, vol. 5, pp. A51–A60, 1993, and references therein.

[36] Y. Nishikawa, A. Tackeuchi, M. Yamaguchi, S. Muto and O. Wada "Ultrafast All-Optical Spin Polarization Switch Using Quantum Well Ethalon", *IEEE Selected topics in Quantum Electron.*, vol. 2, pp. 661–667, 1996.

[37] J. Martin-Regalado, "Polarization Properties of Vertical–Cavity Surface–Emitting lasers," PhD Thesis, Universitat Illes Balears, 1997.

[38] A. Gahl, S. Balle, M. San Miguel, "Polarization properties of optically pumped VCSELs in a transverse magnetic field", *Quantum Semiclass. Opt* **10**, pp. L1–L5, 1998

[39] S. Hallstein, J.D. Berger, M. Hilpert, H.C. Schneider, W.W. Rühle, F. Jahnke, S.W. Koch, H.M. Gibbs, G. Khitrova, and M. Oestreich, "Manifestation of coherent spin precession in stimulated semiconductor emission dynamics," *Phys. Rev. B*, vol. 56, pp. R7076–R7079, 1997.

[40] M. Oestreich, W. W. Rühle, "Spinquantenschwebungen in Halbleitern — der Hanle–Effekt zeitaufgelöst," *Phys. Bl.*, vol. 54, pp. 49–52, 1998.

[41] S. Balle, N.B. Abraham, P. Colet, M. San Miguel, "Parametric Dependence of Stochastic Frequency Variations in the Gain Switching of a Single–Mode Laser Diode", *IEEE J. Quantum Electron.*, vol. 29, pp. 33–41, 1993.

FIGURES

FIG. 1. Model for polarization dynamics in VCSELs (see text).

FIG. 2. a) Polarization resolved PL signals I_+ (full curve) and I_- (dotted curve) after pulsed excitation; b) corresponding spin band populations $N + m_z$ (full curve) and $N - m_z$ (dotted curve); parameters: $\tau = 2\text{ps}$, $\hat{\eta} = 10^{-3}$, $P = 1$, $\gamma = 1\text{ns}^{-1}$, $\beta = 10^{-5}$, $\kappa/\gamma = 10^5$, $\gamma_s/\gamma = 5$, $\gamma_p/\pi = 4\text{GHz}$, $\gamma_a/\gamma_p = 0.01$, $\alpha = 3$, $\Omega_x = 0$.

FIG. 3. a) Polarization resolved PL signals I_+ (full curve) and I_- (dotted curve) after pulsed excitation; b) corresponding spin band populations $N + m_z$ (full curve) and $N - m_z$ (dotted curve); parameters as in Fig. 2 except $\Omega_x/2\pi = 11\text{GHz}$.

FIG. 4. a) Polarization resolved VCSEL emission I_+ (full curve) and I_- (dotted curve) after pulsed excitation; b) corresponding spin band populations $N + m_z$ (full curve) and $N - m_z$ (dotted curve); parameters: $\tau = 2\text{ps}$, $\hat{\eta} = 450$, $P = 0.5$, $\gamma = 1\text{ns}^{-1}$, $\beta = 10^{-5}$, $\kappa/\gamma = 250$, $\gamma_s/\gamma = 5$, $\gamma_p/\pi = 4\text{GHz}$, $\gamma_a/\gamma_p = 0.01$, $\alpha = 3$, $\Omega_x = 0$.

FIG. 5. a) Polarization resolved VCSEL emission I_+ (full curve) and I_- (dotted curve) after pulsed excitation; b) corresponding spin band populations $N + m_z$ (full curve) and $N - m_z$ (dotted curve); parameters as in Fig. 4 except $\Omega_x/2\pi = 11\text{GHz}$.

FIG. 6. Hanle effect in a VCSEL under lasing conditions: ellipticity ϵ of the VCSEL emission versus Larmor frequency Ω_x of the transverse magnetic field; parameters: $\eta = 1.1$, $P = 0.5$, $\gamma = 1\text{ns}^{-1}$, $\kappa/\gamma = 250$, $\gamma_s/\gamma = 100$, $\gamma_p/\pi = 10\text{GHz}$, $\gamma_a = 0$, $\alpha = 3$.

FIG. 7. Time series of the total intensity (dashed curve), the polarization resolved intensities (full curve: I_+, dotted curve: I_-), the magnetization component m_z and the corresponding field spectra (full curve: E_+, dotted curve: E_-); parameters: $\eta = 3$, $\gamma = 1\text{ns}^{-1}$, $\beta = 10^{-5}$, $\kappa/\gamma = 250$, $\gamma_p/\pi = 12\text{GHz}$, $\gamma_a/\gamma_p = 0.01$, $\alpha = 3$, $\Omega_x = 0$; left column: $\gamma_s/\gamma = 150$, $P = 0.9$; right column: $\gamma_s/\gamma = 5$, $P = 0$

FIG. 8. a) Time series of the total intensity; at $t = 0\,\mathrm{ns}$ the pump level is increased from $\eta = 2.00$ to $\eta = 2.12$, at $t = 5\,\mathrm{ns}$ from $\eta = 2.12$ to $\eta = 2.20$; b) field spectra of the transient from $t = 0\,\mathrm{ns}$ to $t = 5\,\mathrm{ns}$ of a) (full curve: E_+, dotted curve: E_-); c) spectra of the stationary fields (full curve: E_+, dotted curve: E_-) for $\eta = 2.20$; other parameters: $P = 0.5$, $\gamma = 1\mathrm{ns}^{-1}$, $\gamma_s/\gamma = 5$, $\beta = 10^{-5}$, $\kappa/\gamma = 250$, $\gamma_p/\pi = 4\mathrm{GHz}$, $\gamma_a/\gamma_p = 0.01$, $\alpha = 3$, $\Omega_x = 0$

FIG. 9. a) Time series of the total intensity (dashed curve) and the polarization resolved intensities (full curve: I_+, dotted curve: I_-); b) Time series of the magnetization components m_z (full curve) and m_y (dotted curve); c) Field spectra corresponding to a); d) Larmor presession in the z–y–plane; parameters: $\eta = 3.5$, $P = 0,\gamma = 1\mathrm{ns}^{-1}$, $\gamma_s/\gamma = 5$, $\beta = 10^{-5}$, $\kappa/\gamma = 250$, $\gamma_p/\pi = 4\mathrm{GHz}$, $\gamma_a/\gamma_p = 0.01$, $\alpha = 3$, $\Omega_x = 11\mathrm{GHz}$

FIG. 10. Dependence of the maximum oscillation frequency $\nu_{\max}$ on the cavity decay rate κ and the pump level η; other parameters as in Fig. 9

Fig. 1

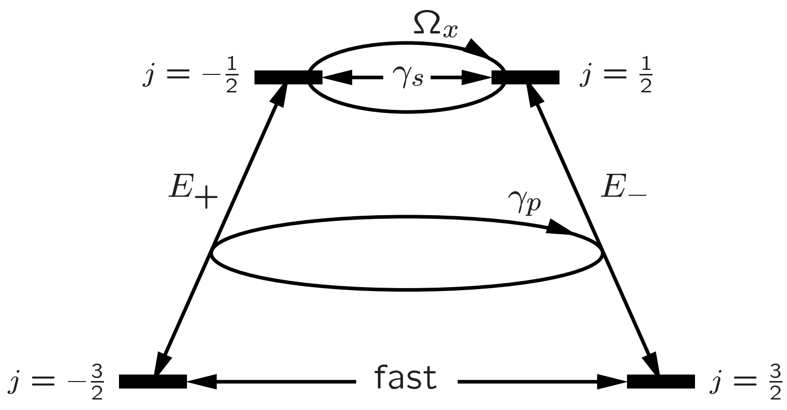

Fig. 2

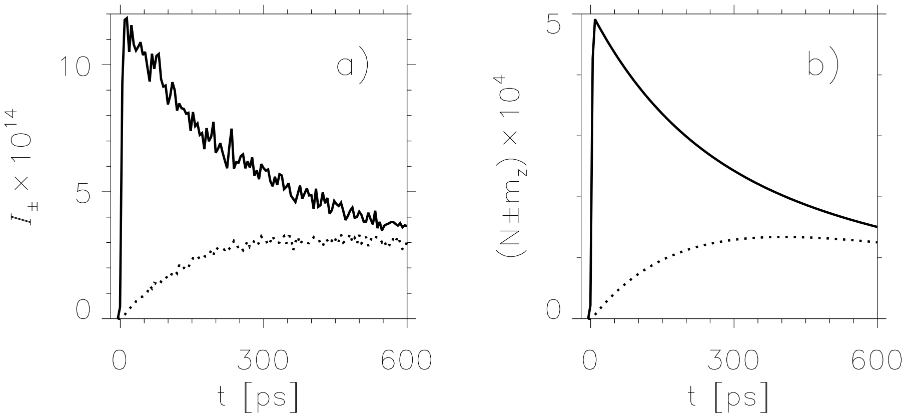
a)
b)
$I_\pm \times 10^{14}$
$(N \pm m_z) \times 10^4$
10
5
0
300
600
t [ps]

Fig. 3

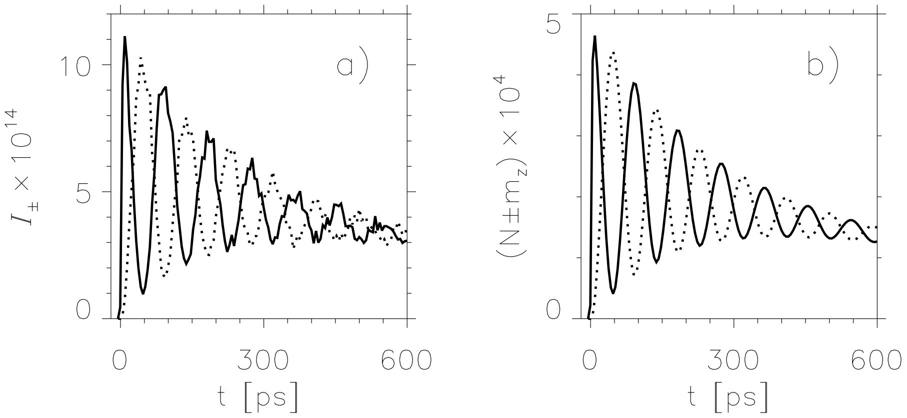
a)
b)
$I_\pm \times 10^{14}$
$(N \pm m_z) \times 10^4$
10
5
0
300
600
t [ps]

Fig. 4

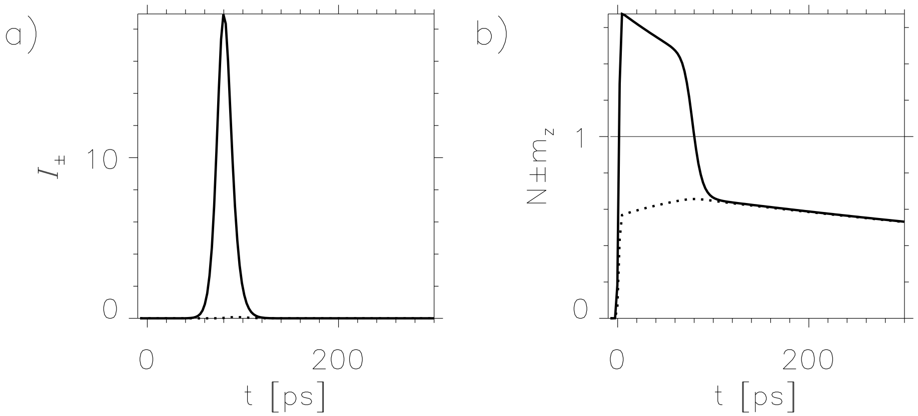
a)
$I_\pm$
0
10
0
200
t [ps]
b)
$N \pm m_z$
0
1
0
200
t [ps]

Fig. 5

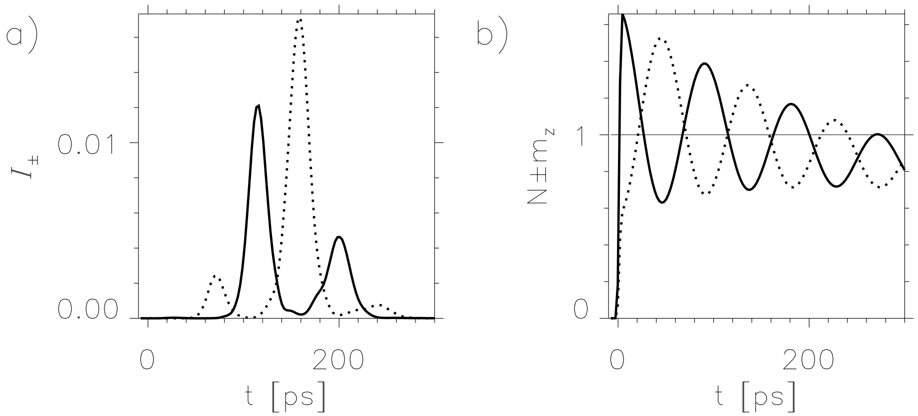
a)
$I_\pm$
0.00
0.01
0
200
t [ps]
b)
$N \pm m_z$
0
1
0
200
t [ps]

Fig. 6

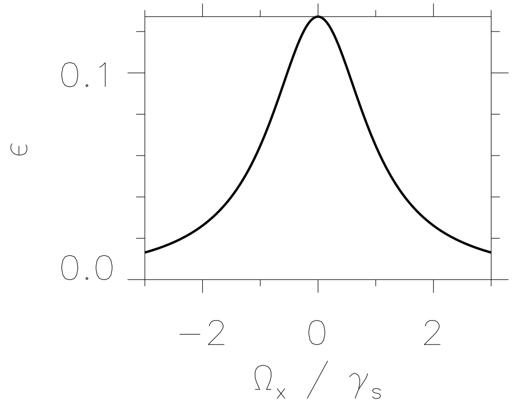

0.1
0.0
ϵ
−2
0
2
Ω_x / γ_s

Fig. 7

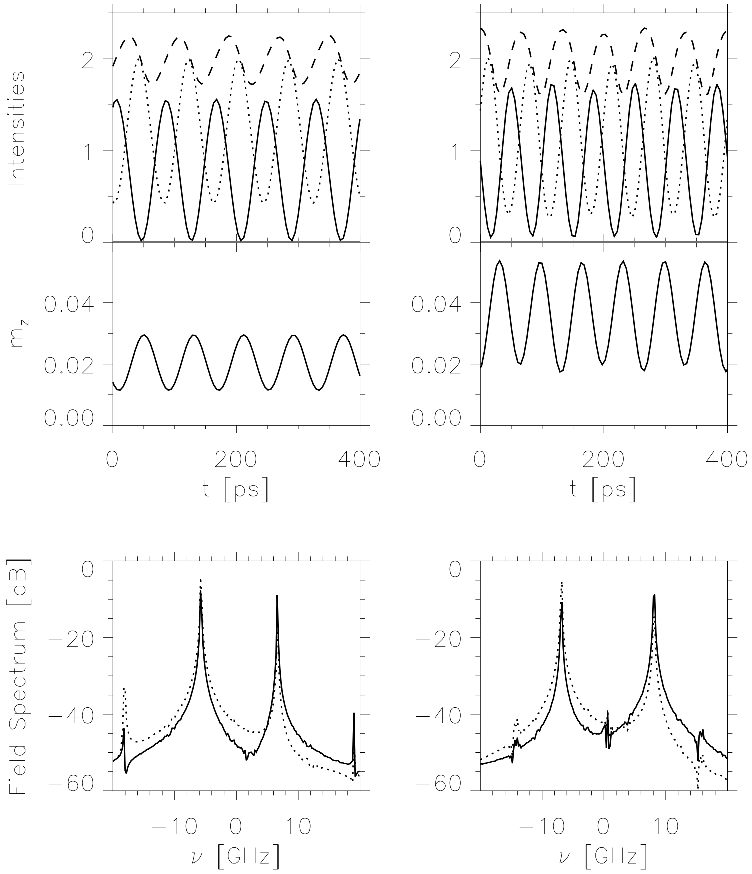

Intensities
m_z
t [ps]
Field Spectrum [dB]
ν [GHz]

Fig. 8

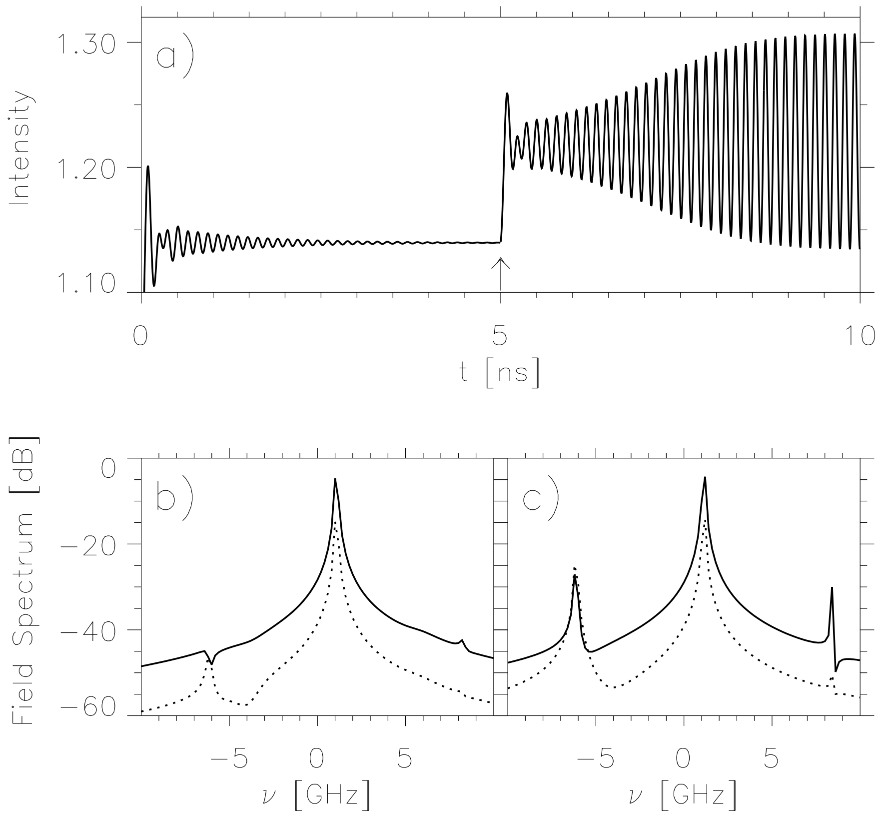
a)
Intensity
1.30
1.20
1.10
0
5
10
t [ns]
b)
c)
Field Spectrum [dB]
0
−20
−40
−60
−5
0
5
ν [GHz]
ν [GHz]

Fig. 9

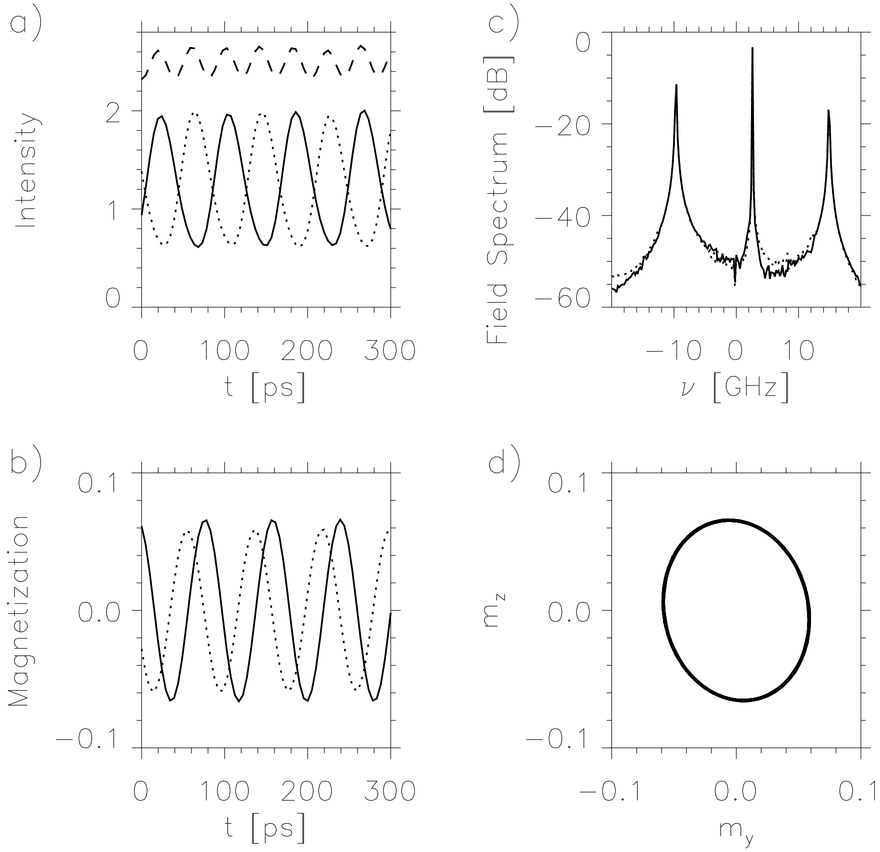
a)
Intensity
2
1
0
0
100
200
300
t [ps]
c)
Field Spectrum [dB]
0
−20
−40
−60
−10
0
10
ν [GHz]
b)
Magnetization
0.1
0.0
−0.1
t [ps]
d)
m_z
m_y

Fig. 10

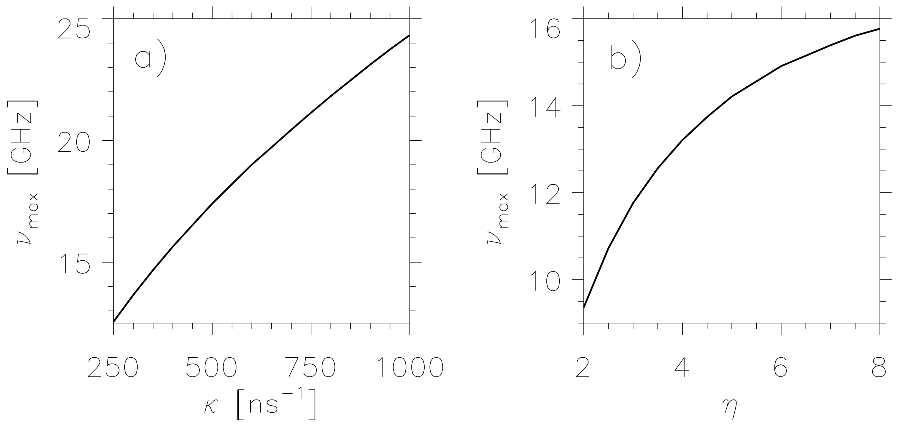

a)
25
20
15
250
500
750
1000
ν_{max} [GHz]
κ [ns^{-1}]
b)
16
14
12
10
2
4
6
8
ν_{max} [GHz]
η